

See discussions, stats, and author profiles for this publication at: <https://www.researchgate.net/publication/278732957>

Perylo[1,12- b , c , d] Thiophene Tetraesters: A New Class of Luminescent Columnar Liquid Crystals

ARTICLE in LANGMUIR · JUNE 2015

Impact Factor: 4.46 · DOI: 10.1021/acs.langmuir.5b01187 · Source: PubMed

READS

27

6 AUTHORS, INCLUDING:



Ravindra Gupta

Indian Institute of Technology Guwahati

5 PUBLICATIONS 7 CITATIONS

[SEE PROFILE](#)



Balaram Pradhan

Indian Institute of Technology Guwahati

3 PUBLICATIONS 2 CITATIONS

[SEE PROFILE](#)



Monika Gupta

Indian Institute of Science Education & Resear...

8 PUBLICATIONS 16 CITATIONS

[SEE PROFILE](#)



Santanu Pal

Indian Institute of Science Education & Resear...

43 PUBLICATIONS 570 CITATIONS

[SEE PROFILE](#)

Perylo[1,12-*b,c,d*] Thiophene Tetraesters: A New Class of Luminescent Columnar Liquid Crystals

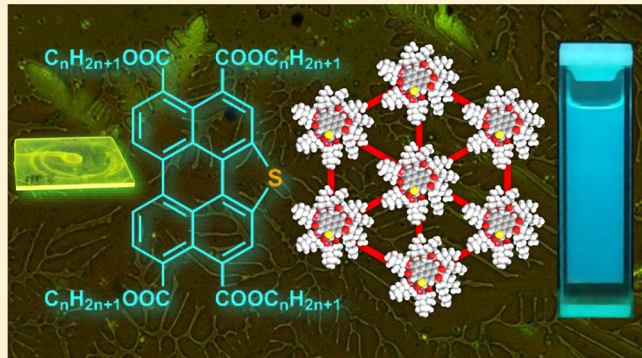
Ravindra Kumar Gupta,[†] Balaram Pradhan,[†] Suraj Kumar Pathak,[†] Monika Gupta,[‡] Santanu Kumar Pal,[‡] and Achalkumar Ammathnadu Sudhakar*,[†]

[†]Department of Chemistry, Indian Institute of Technology Guwahati, Guwahati 781039, Assam, India

[‡]Indian Institute of Science Education and Research, Mohali, Sector-81, Knowledge City, Manauli 140306, Punjab, India

S Supporting Information

ABSTRACT: Perylo[1,12-*b,c,d*] thiophene tetraesters exhibiting wide-range hexagonal columnar phase have been synthesized. These compounds also exhibit good homeotropic alignment in the liquid-crystalline phase which is very important for the device fabrication. These compounds showed sky-blue luminescence in solution under the long-wavelength UV light. With high solubility and high quantum yield these compounds can serve as standards to measure quantum yields of unknown samples. This new class of materials is promising, considering the emissive nature and stabilization of hexagonal columnar mesophase over a wide thermal range and ease of synthesis.



INTRODUCTION

Blue light-emitting materials are receiving increasing attention nowadays because of their inevitable need in producing white light-emitting diodes used for lighting and display applications.¹ White organic light-emitting diodes (WOLEDs) essentially require materials that emit three primary colors, that is, red, blue, and green.² Red- and green-emissive materials are widely reported, but blue-emitting materials are scarce.^{3,4} Even the reported blue-emissive materials usually possess a large band gap, and this leads to inherent drawbacks related to stability, efficiency, and lifetime.³ Mainly three classes of blue-emitting materials are investigated for this purpose, which are based on inorganic semiconductors, emissive polymers, and small organic/metallo-organic molecules. Inorganic semiconductors have disadvantages like high cost, low efficiency, and hazardous nature. Adding to that they cannot be fabricated on a flexible substrate, whereas polymers have this option but suffer from low solubility, purity, and stability, which often leads to low device performance. The advantage of small molecules when compared with the first two classes is that one can synthesize them in large quantity with high purity in a reproducible manner. Small molecules can be vacuum-deposited or spin-coated into high-quality thin films. Among these two techniques, spin coating is an easy and cost-effective way. For spin coating, the material has to be solution processable. Such materials are also compatible for the inexpensive large-scale production by inkjet printing for large area displays.⁴ Inherent charge carrier mobility of these molecules is another factor, which affects the device performance.⁵ This is because in an OLED the opposite charges from the two electrodes undergo

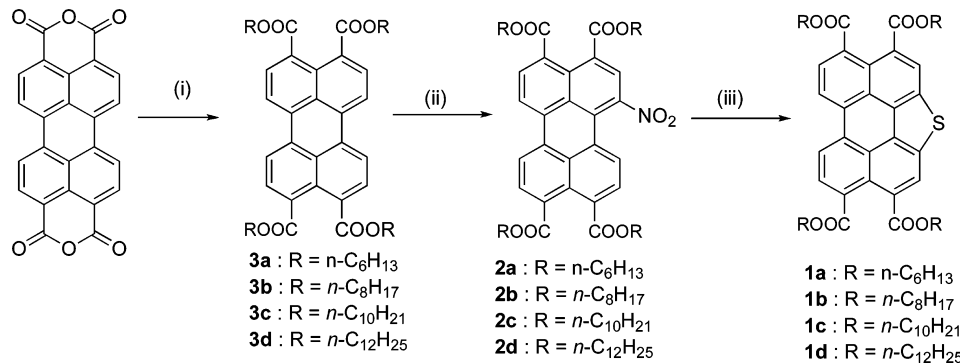
recombination in the emissive layer to generate the light. By appropriate molecular engineering one can direct these molecules to self-assemble into columnar (Col) phases.⁶ Disc-shaped molecules containing a central hard core connected to several flexible chains at the periphery undergo 1D stacking to form Col phases.⁷ Nanosegregation of these incompatible molecular units leads to this 1D stacking, leading to a conducting channel formed by the intimate π -cloud overlap of the individual discs, with an external insulating mantle of alkyl chains. Thus, the Col phases are regarded as molecular wires designed for 1D charge migration.^{8,9} Combining luminescence with Col self-assembly enhances the applicability of the emissive molecules in OLEDs.¹⁰ Flexible alkyl chains in the molecular structure of DLCs also help in the solution processing or ink jet printing. Recently, a few blue light-emitting molecules, which also stabilize Col phases, were reported.^{11–17,24,62}

Perylene derivatives are one of the most sought after class of compounds in the area of organic semiconductors because they are inexpensive, stable (chemical, photochemical, and thermal), and easily functionalizable chromophores with high HOMO–LUMO gap, high molar absorptivity, and high luminescence quantum yield.^{18–20} Hence these materials are widely tested for application in the field of organic photovoltaics (OPVs),^{21,22} OLEDs,²³ and organic field-effect transistors (OFETs).¹⁹ On substituting the central core appropriately these molecules can

Received: April 1, 2015

Revised: June 15, 2015



Scheme 1. Synthesis of S-Annulated Perylene Tetraesters^a

^aReagents and conditions: (i) aqueous KOH solution, 70 °C, 0.5 h, 1M HCl, aliquot 336, KI, *n*-bromoalkanes, reflux, 12 h (69–75%); (ii) NaNO₂, HNO₃, dichloromethane, 0 °C, 1 h (80–90%); (iii) sulfur powder, anhyd. NMP, N₂, 70 °C, 0.5 h, 180 °C, 17 h (55–60%).

aggregate under various conditions and hence are considered to be good candidates in supramolecular chemistry.^{25,26} After Cornier's report on liquid-crystalline (LC) perylene bisimides^{27,28} there were many reports on perylene-bisimide-based liquid crystals derived from aromatic or aliphatic amines. Perylene bisimide LCs with bay substitution were also prepared.^{29–31} Extension along the long axis or in the bay region alters the photophysical properties of perylene bisimides by causing a bathochromic or a hypsochromic shift.³² Bay substitution affects the molecular planarity, photophysical properties, and self-assembly behavior of perylene derivatives.³³ LC perylene tetraesters are a relatively new class of molecules when compared with LC perylenebisimides.³⁴ Perylene tetraesters are comparatively electron rich in comparison with perylene bisimides due to the less electron-withdrawing ester groups. Thus, they can act as good hole-transporting layers, and because of their luminescence properties they can be used as emissive layers in OLEDs.³⁵ Bock et al. reported OLEDs based on perylene tetraesters stabilizing Col_h phase.³⁶ Perylene tetraesters are also known to possess higher HOMO and LUMO levels in comparison with perylene bisimides. This property enhances the open-circuit voltage in solar cells.³⁷

Apart from these two classes, there are not many LC perylene derivatives reported. In particular, bay-modified perylene derivatives are few because a small structural modification in bay region affects the self-assembly and may not support the LC behavior. Bay substitution of hetero atoms like nitrogen and sulfur on incorporation in perylene derivatives led to modified aromatic systems while retaining the planarity.^{38–40} Sun et al. showed that integration of sulfur in the perylene leads to an extraordinary solid state packing due to strong S···S interactions.⁴¹ The field-effect transistor fabricated from the single crystals obtained from these molecules showed a high carrier mobility of 0.8 cm² V⁻¹ s⁻¹. Similarly, Jiang et al. reported the crystalline nanoribbon transistors fabricated from bis-S-annulated perylene, which showed enhanced charge carrier mobility of 2.13 cm² V⁻¹ s⁻¹.⁴² The integration of two sulfur atoms in the perylene molecular structure lead to highly ordered packing, once again due to strong S···S interactions. Mullen's group reported a perylene tetraester with both the bay positions annulated with sulfur;⁴³ however, the photophysical and LC behavior of these compounds was not reported. We anticipated that strong S···S interactions between the S-annulated perlenes would augment the LC self-assembly provided the shape anisotropy is introduced. We considered perylene tetraesters to test our hypothesis because of their

synthetic ease and utility of the annulated products in further modification. In the present work, we are reporting new series of emissive DLCs based on S-annulated perylene tetraesters. This series of molecules is the first report of LC perylene derivatives with sulfur incorporated in their molecular structure and showing blue light emission in solution.

EXPERIMENTAL SECTION

Materials. All commercially obtained chemicals were used as received. As required, the solvents were dried as per the standard protocols. Silica gel or neutral alumina was used as stationary phase for column chromatography. Aluminium sheets coated with silica gel were used for thin layer chromatography (TLC) to monitor the reactions and column purifications.

Measurements and Characterization. Infrared spectra were measured on a PerkinElmer IR spectrometer at room temperature by preparing the KBr pellet. ¹H and ¹³C NMR spectra were recorded using Varian Mercury 400 MHz (at 298 K) or Bruker 600 MHz NMR spectrometer. Mass spectrometry was carried out using MALDI-TOF mass spectrometer or high-resolution mass spectrometer. Polarizing optical microscope (POM) (Nikon Eclipse LV100POL) in conjunction with a controllable hot stage (Mettler Toledo FP90) was used for the characterization of mesogens. The phase transitions and associated enthalpy changes were obtained by differential scanning calorimeter (DSC) (Mettler Toledo DSC1). X-ray diffraction (XRD) studies were carried out using image plate and a detector. This setup had Cu K α ($\lambda = 0.15418$ nm) radiation from a source (GeniX3D, Xenocs) operating at 50 kV and 0.6 mA in conjunction with a multilayer mirror used to irradiate the sample. Glass capillaries containing the sample were used for the measurements. Thermogravimetric analysis (TGA) was accomplished with a thermogravimetric analyzer (Mettler Toledo, model TG/SDTA 851 e). PerkinElmer Lambda 750 UV-vis/NIR spectrometer was used to obtain UV-vis spectra, while Fluoromax-4 fluorescence spectrophotometer and PerkinElmer LS 50B spectrometer were used to obtain emission spectra in solution state and solid thin-film state, respectively. Steady-state anisotropy experiment was performed on Horiba Scientific Fluoromax spectrofluorometer 4. Time-resolved lifetime measurements were done on time-correlated single photon counter from Horiba Jobin Yvon (excitation by 440 nm laser diode). Cyclic voltammetry (CV) studies were carried out using a Versa Stat 3 (Princeton Applied Research) instrument. Atomic force microscopy (AFM) images were obtained for the spin-coated films using Agilent 5500-STM instrument.

Synthesis. Compounds 2b–d and 3b–d were prepared as per the reported procedures.^{44,45} Synthesis of compounds 2a, 3a, and 1a–d is reported in this work. For more details, see the Supporting Information.

RESULTS AND DISCUSSION

Synthesis and Molecular Structural Characterization.

The synthetic scheme to obtain the target DLCs is represented in Scheme 1. Perylene-3,4,9,10-tetracarboxylic bisanhydride converted to their tetraesters **3a–d** and these on nitration yielded nitro compounds **2a–d**.⁴⁴ Compounds **2a–d** were heated with sulfur powder in anhydrous *N*-methylpyrrolidine to yield the target compounds **1a–d** as yellow-orange solids in good yield.⁴⁵ There is a report on bis-S-annulated perylene derivatives prepared by the treatment of tetrachloro derivative of perylene tetraester with bis(tributyltin)sulfide in the presence of tetrakis(triphenylphosphine) palladium (0) catalyst.⁴³ In comparison, this is a simple method with good yield. Structural identity of all of the compounds was established by ¹H, ¹³C NMR, IR spectroscopy, and mass spectrometry. (See the Supporting Information.)

Thermal Behavior. S-annulated perylene tetraesters (**1a–d**) were investigated by POM, DSC, TGA, and XRD studies for their thermal behavior. The transition temperatures and the associated enthalpy changes obtained from the DSC scans of first heating–cooling cycles are tabulated (Table 1). Figure 1

of view under cross-polarizers is due the uniaxial alignment of optical and columnar axis (Figure 2a).^{46,47} The same field of view through parallel polarizers shows hexagonal dendritic domains (Figure 2b). The dendritic branching with a 60° angle to the main axis is depicted in Figure 2b, which is a characteristic for hexagonal columnar (Col_h) phase. In the homeotropic configuration the column axes lie perpendicular to the substrate and thus give the best geometry to visualize the symmetry of the underlying lattice on the substrate plane. The growth of the dendritic structure itself is due to the diffusion of the latent heat across the isotropic to columnar mesophase. The homeotropically aligned Col_h phase is an ideal feature required in the fabrication of organic solar cells.⁴⁹ Incorporation of hetero atoms at the peripheral region of the molecules is known to enhance homeotropic (face-on) alignment over homogeneous alignment (edge-on) on polar surfaces.⁵⁰ In literature, it is also reported that discotic molecules where the core is connected to several flexible tails through ester groups have shown Col_h phase with good homeotropic alignment.^{35,51–55} This is probably due to the intercolumnar dipole–dipole interaction exerted by the ester carbonyl group forcing the efficient correlation of columns over a wide thermal range.⁵³

Further cooling of the mesophase results in a fibrous texture as shown in Figure 2c. This change in the optical texture is only due to the minor change in the alignment of the columns and not due to any mesophase transition, as evidenced from the XRD studies. Finally, the mesophase was crystallized at 62 °C ($\Delta H = 122.1$ kJ/mol, Figure 3a)

Powder XRD measurements were done at temperatures 200 and 100 °C to elucidate mesophase exhibited by compound **1a**. The data obtained on indexing the 1D intensity versus 2θ profile obtained for the Col phases are tabulated in Table 2. The XRD profile of the Col phase (Figure S3a in the SI) at 200 °C showed a sharp reflection corresponding to a Bragg spacing d_{100} at 17.29 Å and another corresponding to a Bragg spacing d_{110} at 10.02 Å. The d spacings corresponding to first two reflections are in the ratio of 1:0.58. Two diffused reflections were found at wide-angle region, one at 4.46 Å and the other at 3.55 Å. First diffused reflection corresponds to the ordering of alkyl chains, while the second diffused reflection corresponds to the ordered packing of rigid cores. All of these features along with the optical textural patterns confirm that the Col phase is having a hexagonal symmetry. From the value of d_{100} one calculates the hexagonal cell parameter “ a ” using the formula $a = d_{100}/\cos 30$ or $2/\sqrt{3} \times d_{100}$, and in this case the value of “ a ” is found to be 19.97 Å. The value of lattice parameter “ a ” calculated was found to be 27% less when compared with the diameter obtained from molecular modeling software (27.38

Table 1. Phase-Transition Temperatures (°C) and Corresponding Enthalpies (kJ/mol) of DLCs^a

compound	phase sequence	
	heating	cooling
1a	Cr ₁ 55.1 (114.4) Cr ₂ 77.4 (117.5) Col _h 235.1 (24.6) I	I 233.1 (23.7) Col _h 62.5 (122.1) Cr
1b	Cr ₁ 65.1 (143) Cr ₂ 81.5 (161.8) Col _h 186.4 (23.3) I	I 185.1 (21.7) Col _h 58.6 (164.2) Cr
1c	Cr ₁ 69.8 (11.5) Cr ₂ 79.3 (462.8) Col _h 148.1 (19.8) I	I 146.4 (18) Col _h 55.4 (196.4) Cr ₂ 23.2 (200) Cr ₁
1d	Cr ₁ 63.1 (68.4) Cr ₂ 85.4 (677) Col _h 112.2 (11.9) I	I 109 (9.9) Col _h 60.3 (232.9) Cr ₂ 43.1 (85.3) Cr ₁

^aPeak temperatures in the DSC thermograms obtained during the first heating and first cooling cycles at 5 °C/min.

summarizes the thermal behavior of these samples in heating cycle. When compared with the parent tetraesters **3a–d**, the compounds **1a–d** show an enhanced mesophase range. Compound **1a** with *n*-hexyloxy tails, exhibited two crystal–crystal (Cr–Cr) transitions before going to form a mesophase at a temperature of 77 °C with an enthalpy change of 117.5 kJ/mol, as noticed in DSC scans. The transition was evidenced with the birefringent sample turning fluidic and shearable. The mesophase was spanning over a broad thermal range of ~157 °C with the isotropic temperature of 235 °C. The isotropic liquid on cooling at 5 °C/min rate showed the homeotropically aligned columnar phase with a dark field of view. The dark field

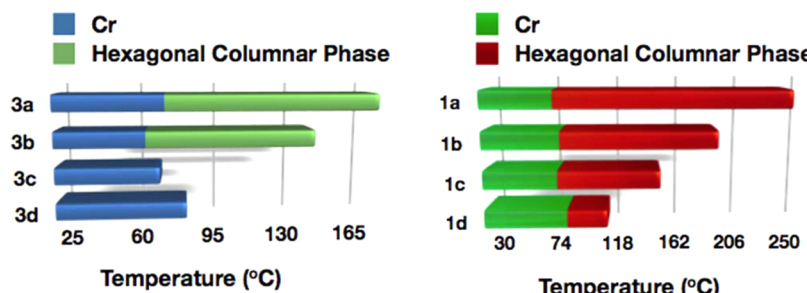


Figure 1. Bar graph showing the thermal behavior of compounds **3a–d**^{34,48} and compounds **1a–d** (heating cycle).

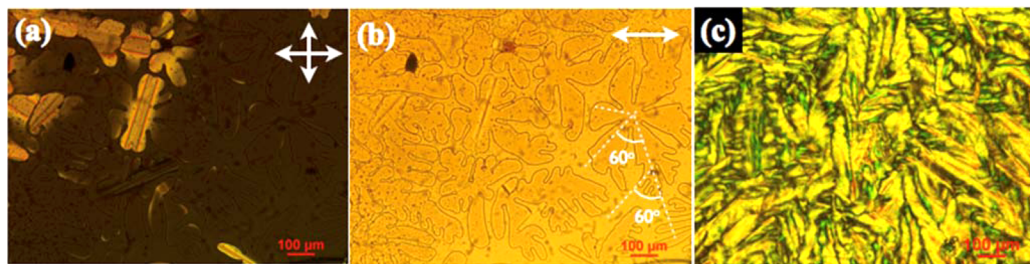


Figure 2. Photomicrograph of compound **1a** at 233 °C (a) as seen under cross polarizers, (b) as seen under parallel polarizers (please note the growth angle), and (c) at 100 °C.

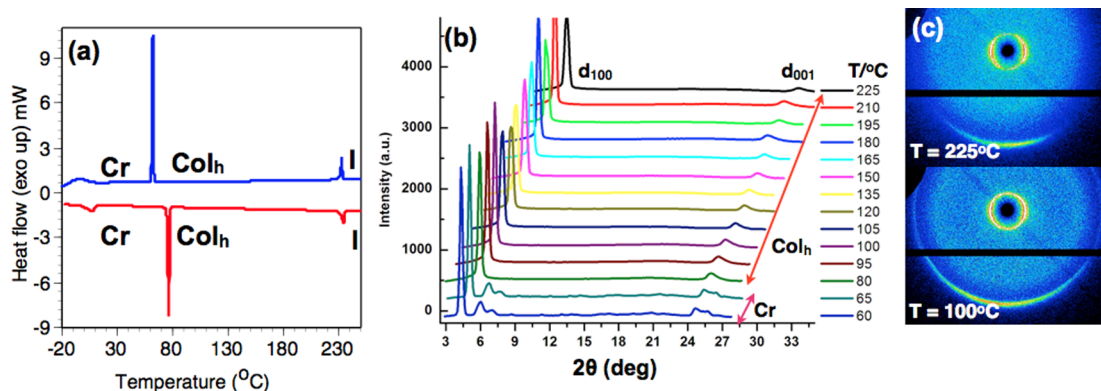


Figure 3. DSC traces for first cooling (blue) and second heating (red) obtained for compounds at a rate of 5 °C/min for compounds **1a** (a). XRD profiles for the compound **1a** as a function of temperature on cooling from isotropic liquid state (b). XRD image patterns obtained at 225 and 100 °C (c).

Table 2. Results of (*hkl*) Indexation of XRD Profiles of the Compounds at a Given Temperature (T) of Mesophases^a

compounds (D/Å)	phase (T/°C)	D _{obs} (Å)	D _{cal} (Å)	Miller indices <i>hkl</i>	lattice parameters (Å), lattice area S (Å ²), molecular volume V (Å ³)
1a (27.38)	200	17.29	17.29	100	<i>a</i> = 19.97; <i>c</i> = 3.55
		10.02	10.03	110	<i>S</i> = 345.1897, <i>V</i> = 1225.42
		4.46 (<i>h_a</i>)			<i>Z</i> = 0.93
		3.55 (<i>h_c</i>)		001	
	100	17.33	17.33	100	<i>a</i> = 20.01; <i>c</i> = 3.54
		10.10	10.05	110	<i>S</i> = 346.7906, <i>V</i> = 1227.64
		4.48 (<i>h_a</i>)			<i>Z</i> = 0.93
		3.54 (<i>h_c</i>)		001	
1b (32.84)	100	18.81	18.81	100	<i>a</i> = 21.72; <i>c</i> = 3.53
		10.97	10.91	110	<i>S</i> = 408.5513, <i>V</i> = 1442.1861
		4.49 (<i>h_a</i>)			<i>Z</i> = 0.96
		3.53 (<i>h_c</i>)		001	
	95	20.5	20.50	100	<i>a</i> = 23.67; <i>c</i> = 3.54
1c (37.38)	95	11.79	11.89	110	<i>S</i> = 485.2637, <i>V</i> = 1717.8355
		10.17	10.25	200	<i>Z</i> = 1.02
		4.56 (<i>h_a</i>)			
		3.54 (<i>h_c</i>)		001	
	90	21.52	21.52	100	<i>a</i> = 24.85; <i>c</i> = 3.49
		12.52	12.48	110	<i>S</i> = 617.4819, <i>V</i> = 1866.2942
		10.85	10.76	200	<i>Z</i> = 0.99
		4.56 (<i>h_a</i>)			
	3.49 (<i>h_c</i>)			001	

^aDiameter (*D*) of the disk (estimated from Chem 3D Pro 8.0 molecular model software from Cambridge Soft). *d_{obs}*: spacing observed; *d_{cal}*: spacing calculated (deduced from the lattice parameters; *a* for Col_h phase; *c* is height of the unit cell). The spacings marked *h_a* and *h_c* correspond to diffuse reflections in the wide-angle region arising from correlations between the alkyl chains and core regions, respectively. *Z* indicates the number of molecules per columnar slice of thickness *h_c* estimated from the lattice area *S* and the volume *V*.

Å). The observed decrease in the value of lattice parameter can be ascribed to the flexible chain folding or their interdigititation in the neighboring columns.^{11,56} The columnar slice thickness

is given by core–core stacking distance, *h_c*, which is 3.55 Å. This is also denoted as the lattice parameter “*c*” for the Col_h phase. The number of molecules “*Z*” filling a unit cell of height

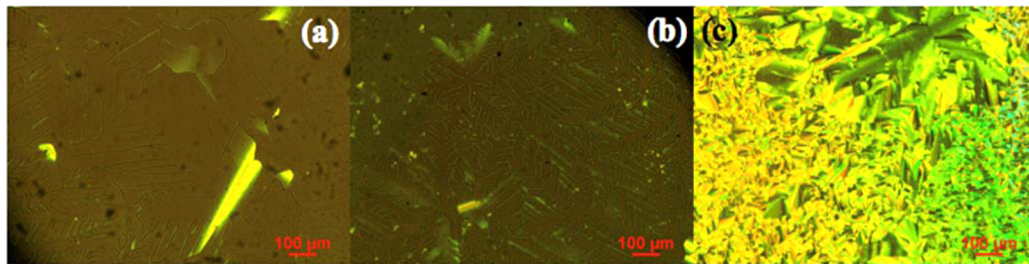


Figure 4. Photomicrographs of compound **1b** at 185 °C (a), **1c** at 146 °C (b), and **1d** at 90 °C (c) on cooling from isotropic liquid state, as seen under cross polarizers.

$h_c = 3.55 \text{ \AA}$ can be calculated from the relation $Z = \delta \times N_A \times V_{\text{unit cell}}/M$. For organic materials, density δ is generally assumed as 1 g/cm³, molecular mass M for **1a** is 795.043 g/mol, and N_A is Avogadro's number. The volume of the hexagonal unit cell is given by the relation: $V_{\text{unit cell}} = S \times h_c$, where S is lattice area, which is calculated using the formula $S = a^2 \times \sin 60$. After substituting all of the values thus obtained (Table 2), the number of molecules filling the columnar slice, that is, Z , is found to be 0.93. This means each stratum in the Col phase is made up of a single molecule and packed in the columns with an intracolumnar distance 3.55 Å. Because the cooling scan in DSC showed a broad thermal range of ~170° and the POM observations also showed a fibrous texture (Figure 2c), we wanted to investigate whether there are any changes in the columnar self-assembly (symmetry of the phase) at low temperature. As seen in Figure 3c and Table 2, the diffraction pattern and data obtained at 100 °C were almost similar to the one obtained at 200 °C with a slight increase in lattice parameter "a" and a slight decrease in core–core distance, h_c . To further confirm that there are no other mesophases except Col_h phase over the entire thermal range, we carried out XRD studies as a function of temperature, starting from 225 to 60 °C (Figure 3b). We observed the strong reflections corresponding to Bragg spacing d_{100} and d_{110} along with the two diffused peaks at wide angle. The ratio of the first two d spacings at low angle corresponds to Col_h phase. Additional reflections are observed at the low- and medium-angle regions; ~65 °C are due to the crystallization.

Higher homologues of this series, that is, compounds **1b**, **1c**, and **1d**, exhibited enantiotropic hexagonal columnar phase with the characteristic optical texture (Figure 4). The mesophase range decreased on going from lower homologue **1a** to higher homologue **1d**. Thus, the increase in the peripheral chain length leads to a lowering of clearing temperatures. TGA analysis showed that these compounds were stable up to ~300 °C, and complete decomposition occurred at ~550 °C (Figure 5).

Photophysical Properties. Photophysical properties of these S-annulated perylene tetraesters are presented in Table 3. Micromolar THF solutions of compounds **1a–d** were used to measure absorption and fluorescence spectra. Representative spectra for compound **1b** are given in Figure 6a. As can be seen, all of the compounds exhibited an absorption maximum centered at 442 nm, with two small shoulders centered at 417 and 398 nm. These molecules showed molar absorption coefficients, which are comparable to the parent perylene tetraester (**1a–d**: $\epsilon = >8930 \text{ M}^{-1} \text{ cm}^{-1}$; **3b**: $\epsilon = 14\,800 \text{ M}^{-1} \text{ cm}^{-1}$). S annulation lead to a hypsochromic shift (~30 nm), in comparison with corresponding parent tetraester **3b** (SI). All of the compounds showed bluish-green fluorescence in solution

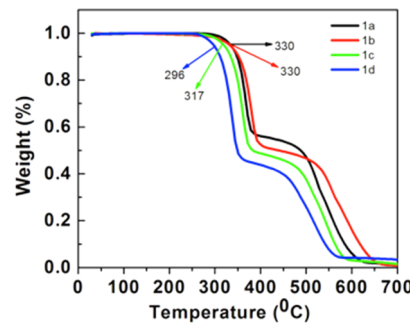


Figure 5. TGA plots of compound **1a–d** (heating rate of 10 °C/min, Nitrogen atmosphere).

even under daylight conditions. Emission spectra of compounds **1a–d** showed the emission maxima centered around 461–464 nm with a shoulder peak at 482 nm. A Stoke's shift of 19–22 nm was observed for these molecules. S-annulated tetraesters exhibit a hypsochromic shift in the absorption and emission maxima when compared with perylene tetraester **3b** (SI), but the value of Stoke's shift was similar to compound **3b**. The length of alkyl chain had no effect on the emission spectra of these molecules in solution.^{48,57,58} Solutions of these compounds exhibit sky-blue fluorescence under UV light of long wavelength, as shown in Figure 6a (inset). It should be noted that tetraester **3b** showed green light emission in solution under the illumination of UV light of 365 nm (Figure S8a (inset) in the SI). Absorption and emission spectra of compound **1b** recorded on dilution from micromolar concentration (SI, Figure S7) suggested that the observed emission is due to the monomer. As a representative case we have measured the quantum yield of compound **1b** with respect to tetrakis(octyl)-1H-phenanthro[1,10,9,8]carbazole-3,4,9,10-tetracarboxylate⁴⁴ (SI). Quantum yield of compound **1b** was found to be 1. Considering the high solubility of compound **1b** in organic solvents and high fluorescence quantum yield, it can be used as a standard for quantum yield measurement (at wavelength 442 nm).⁵⁹

Fluorescence lifetime and steady-state anisotropy measurements were carried out in dilute solutions (3 μM solution in dichloromethane). The measured lifetime for all compounds was found to be ~3 ns (Table 3), which is lower as compared with the measured lifetime value observed for perylene.⁶⁰ The structural variation in terms of size and shape and resulting molecular interaction might lead to higher nonradiative decay, which results in the reduced lifetime. The steady-state anisotropy values showed that compounds **1a–d** are comparable to the previously reported perylene tetraester.⁶¹

Table 3. Photophysical Properties

entry	solution state ^a						thin film ^g		
	absorption (nm)	emission (nm) ^b	Stokes shift nm (cm ⁻¹)	$\Delta E_{g,\text{opt}}^{c,d}$ (eV)	$\tau^{e,f}$ (ns)	steady state anisotropy ^f	absorption (nm)	emission (nm) ^h	Stokes shift nm (cm ⁻¹)
1a	442, 417, 398	461, 481	19 (933)	2.67	3.01	0.024	408, 472	534, 562	126 (5783)
1b	442, 417, 398	464, 482	22 (1073)	2.68	3.05	0.029	408, 471	534	126 (5783)
1c	442, 417, 398	464, 482	22 (1073)	2.68	3.02	0.037	408, 467	542	134 (5060)
1d	442, 417, 398	462, 481	20 (979)	2.68	3.01	0.032	410, 465	538	128 (5803)

^aIn micromolar solutions in THF. ^bExcitation wavelength $\lambda_{\text{ex}} = 442$ nm. ^cCalculated from the absorption onset (465 nm for **1a** and 463 nm for **1b–d**). ^dIn electronvolts. ^eFluorescence lifetime. ^f3 μM solution in dichloromethane. ^gPrepared by the spin-coating of millimolar solution in toluene.

^hExcited at the absorption maxima (408 nm for **1a–c** and 410 nm for **1d**).

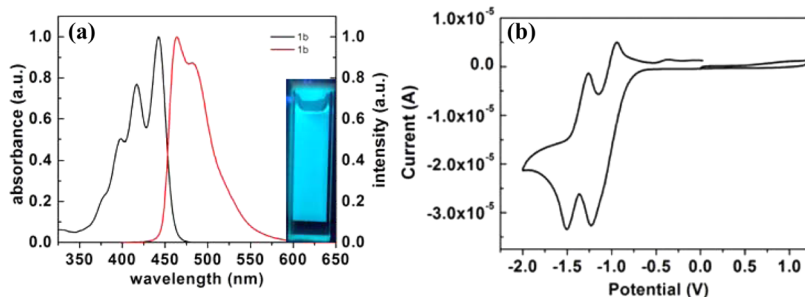


Figure 6. (a) Absorption (LHS) and emission (RHS) spectra in micromolar THF solution for compound **1b**. Inset shows the picture of micromolar THF solutions as seen under the UV illumination of wavelength 365 nm. (b) Cyclic voltammogram of the compound **1b** in anhydrous THF solution of TBAP (0.1 M) at a scanning rate 100 mV/s.

Thin film of compound **1b** was prepared using millimolar solutions of compound in toluene and spin coated on a glass slide. The absorption spectrum obtained for the thin-film showed two maxima at 408 nm with a shoulder at 471 nm, respectively, while the emission spectrum exhibits an emission maximum at 534 nm. The absorption maxima is hypsochromically shifted with respect to that of monomer. The emission spectrum in the solid state was bathochromically shifted (Figure 7). The observed red-shifted emission in the case of

Transition to the lower level is allowed when the molecules in aggregates are arranged in a slip stack fashion (*J* aggregates). Experimentally, this is characterized by a red-shifted absorption band in comparison with the isolated monomer. The blue-shifted absorption maxima in the case of thin film of compound **1b** points to the formation of *H* aggregates, with the molecules being stacked in a cofacial manner within the aggregates.^{63–65} The thin film showed yellowish green luminescence under the UV light of 365 nm wavelength (Figure 7a, inset).

Similarly, thin films of compounds **1a**, **1c**, and **1d** were prepared by spin coating and examined by UV-vis and fluorescence spectroscopy. Compounds **1c** and **1d** showed very similar behavior to compound **1b**, with their absorption and emission spectra being similar (SI). Compound **1a** with hexyloxy chains showed similar absorption spectra, while the emission spectra were having a maximum of 534 nm with a prominent shoulder at 562 nm. Thus, the film showed yellowish orange fluorescence under the UV illumination of 365 nm wavelength. Thus, the chain length has some effect on the emissive properties of these molecules in aggregates, as we have seen in the case of compound **1a** and **1b**, while further increase in the chain length (**1b–d**) does not have any effect. We assume that with the shorter chain length molecular packing will be efficient, thus leading to a red shift in the emission of compound **1a**. We have also annealed the compounds **1a–d** from the isotropic state and taken the absorption and emission spectra. We found that there was not much difference in their photophysical properties (SI). AFM imaging of the thin film revealed the presence of aggregates (Figure 7b). The solid sample in daylight looks bright orange in color, while under UV light of long wavelength (365 nm) it shows yellow emission (Figure S9 in the SI). Sample **1b** sandwiched between two glass coverslips on shearing in its isotropic state formed a thin film of the sample. The characteristic texture for *Col_h* phase was observed on cooling.

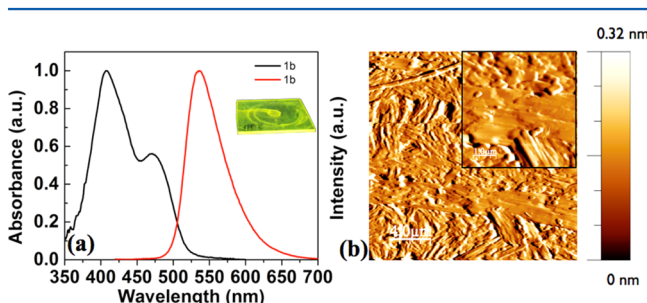


Figure 7. (a) Absorption (black trace) and emission (red trace) spectra obtained for the spin-coated thin film for compound **1b**. (Inset shows the film under UV light of wavelength 365 nm.) (b) AFM topography image of the spin coated film (scale bar is 4 μ m, inset 1 μ m).

thin film is due to the lowered energy level, which is resulted from the close overlap of cores in the thin-film state.⁶² Kasha et al. described that molecular aggregation in the ground state lead to exciton coupling, which, in turn, splits the excited-state aggregates into two energy levels (Davydov splitting).⁶³ When the molecules are stacked one above the other, which are known as *H* aggregates, the transition to the upper level is allowed. A blue-shifted absorption band compared with that of the monomer is the characteristic of this phenomenon.

We tried to freeze the mesophase by subjecting the sample to sudden cooling in the mesophase, but the sample was crystallized. On shining the UV light of 365 nm wavelength, yellowish green fluorescence was observed (SI). This shows emissive nature of the compound in the solid state.

Thus, the compounds in film/solid state show red-shifted emission when compared with their solutions. It is difficult to control the aggregation in thin films because of the planarity of the molecules, but there is a possibility to make good films, which may show the same blue emission in the film state. This can be achieved by mixing these compounds with some nonemissive material. For this, we have to prepare polymerizable S-annulated perylene tetraesters and dope these compounds with some monomer at various concentrations and study their emission properties. Such solutions of optimum concentration can be used for spin coating, followed by polymerization, which may yield good-quality blue-emitting films. The presence of other monomers helps to prevent the aggregation and also helps in cross-linking with emissive monomer for the preparation of polymerized films. Such studies are reported in literature.⁶⁶ The second approach is to modify the molecular design to cause restricted rotation to prevent the molecular aggregation in the film state, but both of these do not guarantee the LC order. Considering the scarcity of blue-emitting molecules we would like to highlight that we have obtained a stable blue-emitting LC material by simple synthetic route, but further structural modifications are required to process them into good-quality films.

Cyclic Voltammetry. Electrochemical properties of S-annulated perylene tetraesters **1a–d** were investigated by CV studies in degassed anhydrous THF solution. The energy levels of frontier orbitals (HOMO and LUMO) obtained from the cyclic voltammograms and experimental conditions are presented in Table 4. S-annulated perylene tetraesters exhibited

Table 4. Electrochemical Properties of S-Annulated Tetraesters^{a,b}

entry	$E_{1\text{red}}^c$	$E_{\text{HOMO}}^{d,e}$	$E_{\text{LUMO}}^{d,f}$	$\Delta E_{\text{g,opt}}^{d,g}$
1a	-1.19	-5.72	-3.05	2.67
1b	-1.23	-5.69	-3.01	2.68
1c	-1.15	-5.76	-3.08	2.68
1d	-1.14	-5.77	-3.09	2.68

^aIn micromolar solutions in THF. ^bExperimental conditions: Ag/AgCl as reference electrode, glassy carbon working electrode, platinum wire counter electrode, TBAP (0.1 M) as a supporting electrolyte, room temperature, and scanning rate 100 mVs⁻¹. ^cIn volts (V). ^dIn electronvolts. ^eEstimated from the formula $E_{\text{HOMO}} = E_{\text{LUMO}} - \Delta E_{\text{g,opt}}$. ^fEstimated from the formula by using $E_{\text{LUMO}} = -[(E_{1\text{red}} - E_{1/2,\text{Fc},\text{Fc}}^+) + 4.8]$ eV. ^gCalculated from the red edge of the absorption band (465 nm for **1a** and 463 nm for **1b–d**).

an optical band gap of ~2.68 eV. Energy levels of HOMO and LUMO were estimated from the formulas $E_{\text{HOMO}} = E_{\text{LUMO}}$ eV $- \Delta E_{\text{g,opt}}$ and $E_{\text{LUMO}} = -[(E_{1\text{red}} - E_{1/2,\text{Fc},\text{Fc}}^+) + 4.8]$ eV.^{67,68} The HOMO and LUMO levels were found to be around -5.7 and -3.1 eV. When compared with the perylene tetraester **3b**, the bandgap was found to be higher in the case of S-annulated tetraesters. The HOMO level and LUMO levels of **3b** were found to be -5.14 and -2.91 eV, respectively, with an optical bandgap of 2.46 eV. Thus, in the case of S-annulated tetraesters, HOMO and LUMO levels were lowered and bandgap increased, which is a result of the sulfur annulation. We have

also measured the CV of other homologues and found that there is not much effect of chain length on the electrochemical behavior of these compounds.

CONCLUSIONS

Perylo[1,12-*b,c,d*] thiophene tetraesters are a promising class of discotics liquid crystals with good thermal and photophysical behavior. They self-assemble to form an ordered hexagonal columnar phase with broad thermal range and good homeotropic alignment. The columnar packing involves the folding or interdigitation of the peripheral alkyl tails, as evidenced from lower value of the hexagonal lattice parameter in comparison with molecular diameter. With the increase in the flexible chain length the mesophase range is curtailed due to the reduction in the clearing temperature. These molecules show visually perceivable sky-blue light emission in solution with a high quantum yield. These molecules also can be used as standards to measure the quantum yields of unknown compounds owing to their high solubility. The length of the alkyl chains had no effect on the absorption and emission properties in solution state. In the thin-film state, except for the compound with four hexyloxy chains, other homologues showed similar emission behavior. CV studies have shown that S annulation lowers the HOMO and LUMO levels with the concomitant increase in the band gap with respect to the parent perylene tetraesters. Variation in the chain length does not affect their electrochemical behavior. In essence, this series of molecules are promising with respect to their photophysical properties, self-assembly behavior, and the potential for the fabrication of OLEDs.

ASSOCIATED CONTENT

Supporting Information

Synthesis and characterization details, ¹H NMR and ¹³C NMR spectra of all new compounds, absorption and emission spectra, POM photographs, DSC thermograms, XRD profiles of LC compounds, TGA curves, and cyclic voltammograms. The Supporting Information is available free of charge on the ACS Publications website at DOI: 10.1021/acs.langmuir.5b01187.

AUTHOR INFORMATION

Corresponding Author

*E-mail: achalkumar78@gmail.com; achalkumar@iitg.ernet.in. Fax: +91-361-258-2349. Tel: +91-361-258-2329.

Notes

The authors declare no competing financial interest.

ACKNOWLEDGMENTS

A.A.S. sincerely thanks Science and Engineering Board (SERB), DST, Govt. of India, and BRNS-DAE for funding this work through the project no. SB/S1/PC-37/2012 and no. 2012/34/31/BRNS/1039, respectively. We thank Ministry of Human Resource Development for Centre of Excellence in FAST (F. No. 5-7/2014-TS-VII). A.A.S. acknowledges CIF, IIT Guwahati for analytical facilities. We acknowledge Dr. Chandan Mukherjee for providing his Electrochemical workstation. S.K.P. sincerely thanks Department of Science and Technology, Key Project SR/FT/CS-47/2011.

REFERENCES

- (1) Gather, M. C.; Köhnen, A.; Meerholz, K. White organic light-emitting diodes. *Adv. Mater.* **2011**, *23*, 233–248.

- (2) Xiao, L.; Chen, Z.; Qu, B.; Luo, J.; Kong, S.; Gong, Q.; Kido, J. Recent progresses on materials for electrophosphorescent organic light-emitting devices. *Adv. Mater.* **2011**, *23*, 926–952.
- (3) Tong, Q. X.; Lai, S. L.; Chan, M. Y.; Zhou, Y. C.; Kwong, H. L.; Lee, C. S.; Kwon, O. A High performance nondoped blue organic light-emitting device based on a diphenylfluoranthene-substituted fluorene derivative. *J. Phys. Chem. C* **2009**, *113* (15), 6227–6230.
- (4) Ashenhurst, J.; Brancaleon, L.; Gao, S.; Liu, W.; Schmider, H.; Wang, S.; Wu, G.; Wu, Q. G. Blue luminescent organoaluminum compounds: $\text{Al}(\text{CH}_3)_2(\text{dpa})$, $\text{Al}_2(\text{CH}_3)_5(\text{dpa})_2$, $\text{Al}_4(\text{O})_2(\text{CH}_3)_6(\text{dpa})_2$, and $\text{Al}(\text{pfap})_3$, dpa = deprotonated di-2-pyridylamine, pfap = deprotonated 2-pentafluoroanilinopyridine. *Organometallics* **1998**, *17*, S334–S341.
- (5) O'Neill, M.; Kelly, S. M. Ordered materials for organic electronics and photonics. *Adv. Mater.* **2011**, *23*, 566–584.
- (6) Chandrasekhar, S.; Sadashiva, B. K.; Suresh, K. A. Liquid crystals of disc-like molecules. *Pramana* **1977**, *9*, 471–480.
- (7) Li, Q. *Nanoscience with Liquid Crystals: From Self-Organized Nano-Structures to Applications*; Springer: Heidelberg, 2014.
- (8) Li, Q. *Self-Organized Organic Semiconductors: From Materials to Device Applications*; John Wiley & Sons: Hoboken, NJ, 2011.
- (9) Li, Q. *Liquid Crystals beyond Displays: Chemistry, Physics, And Applications*; John Wiley & Sons: Hoboken, NJ, 2012.
- (10) Bock, H.; von Seggern, H.; Bechtold, I. H. Order induced charge carrier mobility enhancement in columnar liquid crystal diodes. *ACS Appl. Mater. Interfaces* **2013**, *5*, 11935–11943.
- (11) Pathak, S. K.; Gupta, R. K.; Nath, S.; Rao, D. S. S.; Prasad, S. K.; Achalkumar, A. S. Columnar self-assembly of star-shaped luminescent oxadiazole and thiadiazole derivatives. *J. Mater. Chem. C* **2015**, *3*, 2940–2952.
- (12) Cristiano, R.; Eccher, J.; Bechtold, I. H.; Tironi, C. N.; Vieira, A. A.; Molin, F.; Gallardo, H. Luminescent columnar liquid crystals based on tristriazolotriazine. *Langmuir* **2012**, *28*, 11590–11598.
- (13) Cristiano, R.; Gallardo, H.; Bortoluzzi, A. J.; Bechtold, I. H.; Campos, C. E. M.; Longo, R. L. Tristriazolotriazines: a core for luminescent discotic liquid crystals. *Chem. Commun.* **2008**, *41*, 5134–5136.
- (14) Girotto, E.; Eccher, J.; Vieira, A. A.; Bechtold, I. H.; Gallardo, H. Luminescent columnar liquid crystals based on 1,3,4-oxadiazole. *Tetrahedron* **2014**, *70*, 3355–3360.
- (15) Cristiano, R.; Gallardo, H.; Bortoluzzi, A. J.; Bechtold, I. H.; Campos, C. E. M.; Longo, R. L. Tristriazolotriazines: a core for luminescent discotic liquid crystals. *Chem. Commun.* **2008**, 5134–5136.
- (16) Ferreira, M.; Girotto, E.; Bentaleb, A.; Hillard, E. A.; Gallardo, H.; Durola, F.; Bock, H. Columnar liquid-crystalline dinaphthoperylene-tricarboxylic diimides. *Chem.—Eur. J.* **2015**, *21*, 4391–4397.
- (17) Stefan, G.; Thorsten, R.; Borchmann, D.; Fortunati, I.; Signorini, R.; Detert, H. Arylethynyl-substituted tristriazolotriazines: synthesis, optical properties, and thermotropic behavior. *Eur. J. Org. Chem.* **2014**, *15*, 3116–3126.
- (18) Grimsdale, A. C.; Chan, K. L.; Martin, R. E.; Jokisz, P. G.; Holmes, A. B. Synthesis of light-emitting conjugated polymers for applications in electroluminescent devices. *Chem. Rev.* **2009**, *109*, 897–1091.
- (19) Malenfant, P. R. L.; Dimitrakopoulos, C. D.; Gelorme, J. D.; Kosbar, L. L.; Graham, T. O.; Curioni, A. N-type organic thin-film transistor with high field-effect mobility based on a N,N' -dialkyl-3,4,9,10-perylene tetracarboxylic diimide derivative. *Appl. Phys. Lett.* **2002**, *80*, 2517–2519.
- (20) Würthner, F.; Bauer, C.; Stepanenko, V.; Yagai, S. A black perylene bisimide super gelator with an unexpected j-type absorption band. *Adv. Mater.* **2008**, *20*, 1695–1698.
- (21) Peumans, P.; Uchida, S.; Forrest, S. R. Efficient bulk heterojunction photovoltaic cells using small-molecular-weight organic thin films. *Nature* **2003**, *425*, 158–162.
- (22) Li, C.; Liu, M.; Pschirer, N. G.; Baumgaten, M.; Müllen, K. Polyphenylene-based materials for organic photovoltaics. *Chem. Rev.* **2010**, *110*, 6817–6855.
- (23) Grimsdale, A. C.; Chan, K. L.; Martin, R. E.; Jokisz, P. G.; Holmes, A. B. Synthesis of light-emitting conjugated polymers for applications in electroluminescent devices. *Chem. Rev.* **2009**, *109*, 897–1091.
- (24) Yelamaggad, C. V.; Achalkumar, A. S.; Rao, D. S. S.; Prasad, S. K. Luminescent, liquid crystalline tris(*n*-salicylideneaniline)s: synthesis and characterization. *J. Org. Chem.* **2009**, *74*, 3168–3171.
- (25) Würthner, F.; Thalacker, C.; Sautter, A. Hierarchical organization of functional perylene chromophores to mesoscopic superstructures by hydrogen bonding and π – π interactions. *Adv. Mater.* **1999**, *11*, 754–758.
- (26) Xue, C.; Gutierrez-Cuevas, K.; Gao, M.; Urbas, A.; Li, Q. Photomodulated self-assembly of hydrophobic thiol monolayer-protected gold nanorods and their alignment in thermotropic liquid crystal. *J. Phys. Chem. C* **2013**, *117*, 21603–21608.
- (27) Cornier, R. A.; Gregg, B. A. Self-organization in thin films of liquid crystalline perylene diimides. *J. Phys. Chem. B* **1997**, *101*, 11004–11006.
- (28) Cornier, R. A.; Gregg, B. A. Synthesis and characterization of liquid crystalline perylene diimides. *Chem. Mater.* **1998**, *10*, 1309–1319.
- (29) Struijk, C. W.; Sieval, A. B.; Dakhorst, J. E. J.; van Dijk, M.; Kimkes, P.; Koehorst, R. B. M.; Donker, H.; Schaafsma, T. J.; Picken, S. J.; van de Craats, A. M.; Warman, J. M.; Zuilhof, H.; Sudhölter, E. J. R. Liquid crystalline perylene diimides: architecture and charge carrier mobilities. *J. Am. Chem. Soc.* **2000**, *122*, 11057–11066.
- (30) Würthner, F.; Thalacker, C.; Diele, S.; Tschierske, C. Fluorescent J-type aggregates and thermotropic columnar mesophases of perylene bisimide dyes. *Chem.—Eur. J.* **2001**, *7*, 2245–2253.
- (31) Jancy, B.; Asha, S. K. Control of molecular structure in the generation of highly luminescent liquid crystalline perylenebisimide derivatives: synthesis, liquid crystalline and photophysical properties. *Chem. Mater.* **2008**, *20*, 169–181.
- (32) Jiang, W.; Qian, H.; Li, Y.; Wang, Z. Heteroatom-annulated perylenes: practical synthesis, photophysical properties, and solid-state packing arrangement. *J. Org. Chem.* **2008**, *73*, 7369–7372.
- (33) Schmidt, R.; Ling, M. M.; Oh, J. H.; Winkler, M.; Konemann, M.; Bao, Z.; Würthner, F. Core-fluorinated perylene bisimide dyes: air stable n-channel organic semiconductors for thin film transistors with exceptionally high on-to-off current ratios. *Adv. Mater.* **2007**, *19*, 3692–3695.
- (34) Benning, S.; Kitzerow, H.-S.; Bock, H.; Achard, M.-F. Fluorescent columnar liquid crystalline 3,4,9,10-tetra-(*n*-alkoxycarbonyl)-perlenes. *Liq. Cryst.* **2000**, *27*, 901–906.
- (35) Hassieder, T.; Benning, S. A.; Kitzerow, H.-S.; Achard, M.-F.; Bock, H. Color-tuned electroluminescence from columnar liquid crystalline alkyl arenecarboxylates. *Angew. Chem., Int. Ed.* **2001**, *40*, 2060–2063.
- (36) Seguy, I.; Destruel, P.; Bock, H. An all-columnar bilayer light-emitting diode. *Synth. Met.* **2000**, *111*, 15–18.
- (37) Jiang, Y.; Lu, L.; Yang, M.; Zhan, C.; Xie, Z.; Verpoort, F.; Xiao, S. Taking the place of perylene diimide: perylene tetracarboxylic tetraester as a building block for polymeric acceptors to achieve higher open circuit voltage in all-polymer bulk heterojunction solar cells. *Polym. Chem.* **2013**, *4*, 5612–5620.
- (38) Qian, H.; Liu, C.; Wang, Z.; Zhu, D. S-heterocyclic annelated perylene bisimide: synthesis and co-crystal with pyrene. *Chem. Commun.* **2006**, 4587–4589.
- (39) Qian, H.; Yue, W.; Zhen, Y.; Di Motta, S.; Di Donato, E.; Negri, F.; Qu, J.; Xu, W.; Zhu, D.; Wang, Z. Heterocyclic annelated di(perylene bisimide): constructing bowl-shaped perylene bisimides by the combination of steric congestion and ring strain. *J. Org. Chem.* **2009**, *74*, 6275–6282.
- (40) Jiang, W.; Li, Y.; Wang, Z. Heteroarenes as high performance organic semiconductors. *Chem. Soc. Rev.* **2013**, *42*, 6113–6127.
- (41) Sun, Y.; Tan, L.; Jiang, S.; Qian, H.; Wang, Z.; Yan, D.; Di, C.; Wang, Y.; Wu, W.; Yu, G.; Yan, S.; Wang, C.; Hu, W.; Liu, Y.; Zhu, D. High-performance transistor based on individual single-crystalline

- micrometer wire of perylo[1,12-*b,c,d*]thiophene. *J. Am. Chem. Soc.* **2007**, *129*, 1882–1883.
- (42) Jiang, W.; Zhou, Y.; Geng, H.; Jiang, S.; Yan, S.; Hu, W.; Wang, Z.; Shuai, Z.; Pei, J. Solution-processed, high-performance nanoribbon transistors based on dithioperylene. *J. Am. Chem. Soc.* **2011**, *133*, 1–3.
- (43) Zagranjarski, Y.; Chen, L.; Jänsch, D.; Gessner, T.; Li, C.; Müllen, K. Toward perylene dyes by the hundsdiecker reaction. *Org. Lett.* **2014**, *16*, 2814–2817.
- (44) Gupta, R. K.; Pathak, S. K.; Pradhan, B.; Rao, D. S. S.; Prasad, S. K.; Achalkumar, A. S. Self-assembly of luminescent *N*-annulated perylene tetraesters into fluid columnar phases. *Soft Matter* **2015**, *11*, 3629–3636.
- (45) Jiang, W.; Qian, H.; Li, Y.; Wang, Z. heteroatom-annulated perylenes: practical synthesis, photophysical properties, and solid-state packing arrangement. *J. Org. Chem.* **2008**, *73*, 7369–7372.
- (46) Lee, J. J.; Yamaguchi, A.; Alam, M. A.; Yamamoto, Y.; Fukushima, T.; Kato, K.; Takata, M.; Fujita, N.; Aida, T. Discotic ionic liquid crystals of triphenylene as dispersants for orienting single-walled carbon nanotubes. *Angew. Chem., Int. Ed.* **2012**, *51*, 8490–8494.
- (47) Laschat, S.; Baro, A.; Steinke, N.; Giesselmann, F.; Hagele, C.; Scalia, G.; Judele, R.; Kapatsina, E.; Sauer, S.; Schreivogel, A.; Tosoni, M. Discotic liquid crystals: from tailor-made synthesis to plastic electronics. *Angew. Chem., Int. Ed.* **2007**, *46*, 4832–4837.
- (48) Mo, X.; Chen, H.-Z.; Shi, M.-M.; Wang, M. Syntheses and aggregate behaviors of liquid crystalline alkoxy carbonyl substituted perylenes. *Chem. Phys. Lett.* **2006**, *417*, 457–460.
- (49) Simpson, C. D.; Wu, J.; Watson, M. D.; Mullen, K. From graphite molecules to columnar superstructures – an exercise in nanoscience. *J. Mater. Chem.* **2004**, *14*, 494–504.
- (50) Eccher, J.; Faria, G. C.; Bock, H.; von Seggern, H.; Bechtold, I. H. Order induced charge carrier mobility enhancement in columnar liquid crystal diodes. *ACS Appl. Mater. Interfaces* **2013**, *5*, 11935–11943.
- (51) Bock, H.; Rajaoarivelio, M.; Clavaguera, S.; Grelet, E. An efficient route to stable room-temperature liquid-crystalline triphenylenes. *Eur. J. Org. Chem.* **2006**, *13*, 2889–2893.
- (52) Grelet, E.; Dardel, S.; Bock, H.; Goldmann, M.; Lacaze, E.; Nallet, F. Morphology of open films of discotic hexagonal columnar liquid crystals as probed by grazing incidence X-ray diffraction. *Eur. Phys. J. E* **2010**, *31*, 343–349.
- (53) Osawa, T.; Kajitani, T.; Hashizume, D.; Ohsumi, H.; Sasaki, S.; Takata, M.; Koizumi, Y.; Saeki, A.; Seki, S.; Fukushima, T.; Aida, T. Wide-range 2d lattice correlation unveiled for columnarly assembled triphenylene hexacarboxylic esters. *Angew. Chem., Int. Ed.* **2012**, *51*, 7990–7993.
- (54) Zhou, X.; Kang, S. W.; Kumar, S.; Kulkarni, R. R.; Cheng, S. D. Z.; Li, Q. Self-assembly of porphyrin and fullerene supramolecular complex into highly ordered nanostructure by simple thermal annealing. *Chem. Mater.* **2008**, *20*, 3551–3553.
- (55) Li, L.; Kang, S. W.; Harden, J.; Sun, Q.; Zhou, X.; Dai, L.; Jakli, A.; Kumar, S.; Li, Q. Nature-inspired light-harvesting liquid crystalline porphyrins for organic photovoltaics. *Liq. Cryst.* **2008**, *35* (3), 233–239.
- (56) Percec, V.; Ahn, C.-H.; Bera, T. K.; Ungar, G.; Yeardley, D. J. P. Coassembly of a hexagonal columnar liquid crystalline superlattice from polymer(s) coated with a three-cylindrical bundle supramolecular dendrimer. *Chem.—Eur. J.* **1999**, *5*, 1070–1083.
- (57) Uznanski, P.; Marguet, S.; Markovitsi, D.; Schuhmacher, P.; Ringsdorf, H. Photophysical properties of discotic dibenzopyrenes. *Mol. Cryst. Liq. Cryst.* **1997**, *293*, 123–133.
- (58) Yelamaggad, C. V.; Achalkumar, A. S.; Rao, D. S. S.; Prasad, S. K. Luminescent, liquid crystalline tris(*n*-salicylideneaniline)s: synthesis and characterization. *J. Org. Chem.* **2009**, *74*, 3168–3171.
- (59) Brouwer, A. M. Standards for photoluminescence quantum yield measurements in solution. *Pure Appl. Chem.* **2011**, *83* (12), 2213–2228.
- (60) Johansson, L. B.-Å.; Langhals, H. Spectroscopic studies of fluorescent perylene dyes. *Spectrochim. Acta* **1991**, *47A*, 857–861.
- (61) Gupta, S. K.; Setia, S.; Sidiq, S.; Gupta, M.; Kumar, S.; Pal, S. K. New perylene-based non-conventional discotic liquid crystals. *RSC Adv.* **2013**, *3*, 12060–12065.
- (62) Achalkumar, A. S.; Hiremath, U. S.; Rao, D. S. S.; Prasad, S. K.; Yelamaggad, C. V. Self-Assembly of hekates-tris(*N*-salicylideneaniline)s into columnar structures: synthesis and characterization. *J. Org. Chem.* **2013**, *78*, 527–544.
- (63) Kasha, M.; Rawls, H. R.; El-Bayoumi, M. A. The exciton model in molecular spectroscopy. *Pure Appl. Chem.* **1965**, *11*, 371–392.
- (64) Prabhu, D. D.; Sivadas, A. P.; Das, S. Solvent assisted fluorescence modulation of a C_3 -symmetric organogelator. *J. Mater. Chem. C* **2014**, *2*, 7039–7046.
- (65) Spano, F. C. The spectral signatures of Frenkel polarons in H- and J-aggregates. *Acc. Chem. Res.* **2010**, *43*, 429–439.
- (66) Sonawane, S. L.; Asha, S. K. Blue, green, and orange-red emission from polystyrene microbeads for solid-State white-light and multicolor emission. *J. Phys. Chem. B* **2014**, *118*, 9467–9475.
- (67) Li, Y.; Cao, Y.; Gao, J.; Wang, D.; Yu, G.; Heeger, A. J. Electrochemical properties of luminescent polymers and polymer light-emitting electrochemical cells. *Synth. Met.* **1999**, *99*, 243–248.
- (68) Yelamaggad, C. V.; Achalkumar, A. S.; Rao, D. S. S.; Prasad, S. K. Monodispersive linear supermolecules stabilizing unusual fluid layered phases. *Org. Lett.* **2007**, *9*, 2641–2644.